The Journal of Chemical Physics

# Surface hopping with a manifold of electronic states. II. Application to the many-body Anderson-Holstein model

Cite as: J. Chem. Phys. **142**, 084110 (2015); https://doi.org/10.1063/1.4908034
Submitted: 05 December 2014 • Accepted: 01 February 2015 • Published Online: 25 February 2015

Wenjie Dou, Abraham Nitzan and Joseph E. Subotnik

# Surface hopping with a manifold of electronic states. II. Application to the many-body Anderson-Holstein model

Wenjie Dou,[1] Abraham Nitzan,[2] and Joseph E. Subotnik[1]
[1]*Department of Chemistry, University of Pennsylvania, Philadelphia, Pennsylvania 19104, USA*
[2]*School of Chemistry, The Sackler Faculty of Science, Tel Aviv University, Tel Aviv 69978, Israel*

(Received 5 December 2014; accepted 1 February 2015; published online 25 February 2015)

We investigate a simple surface hopping (SH) approach for modeling a single impurity level coupled to a single phonon and an electronic (metal) bath (i.e., the Anderson-Holstein model). The phonon degree of freedom is treated classically with motion along–and hops between–diabatic potential energy surfaces. The hopping rate is determined by the dynamics of the electronic bath (which are treated implicitly). For the case of one electronic bath, in the limit of small coupling to the bath, SH recovers phonon relaxation to thermal equilibrium and yields the correct impurity electron population (as compared with numerical renormalization group). For the case of out of equilibrium dynamics, SH current-voltage (I-V) curve is compared with the quantum master equation (QME) over a range of parameters, spanning the quantum region to the classical region. In the limit of large temperature, SH and QME agree. Furthermore, we can show that, in the limit of low temperature, the QME agrees with real-time path integral calculations. As such, the simple procedure described here should be useful in many other contexts. © *2015 AIP Publishing LLC.* [http://dx.doi.org/10.1063/1.4908034]

## I. INTRODUCTION

Surface hopping (SH) has proven to be a very successful approach for treating nuclear-electronic coupling.[1,2] When it began in 1971, the most basic idea of Tully-Preston surface hopping was to propagate classical nuclei, while switching the active force field whenever nuclei move through avoided crossings.[2] Later, Tully extended the notion of hopping at crossings to a continuous probability of hopping that was calculated at every time step (e.g., the so-called "Fewest Switches Surface Hopping" (FSSH)[1]). More recently, there has been a great deal of theoretical work trying to fix up the decoherence failures of the FSSH algorithm[3–22] and to extract spectroscopic information from SH trajectories.[23–27] There has also been a great amount of work exploring the foundations of the SH approach[28] vis-a-vis the quantum classical Liouville equation.[29–32]

As applied in the literature, SH has been used to model a host of experimental systems, including energy transfer,[33] proton-coupled electron transfer,[34] and electronic relaxation.[35] Of particular interest to this article are the recent studies by Tretiak[36] and Prezhdo,[37] who have studied energy transfer in extended organic chromophores and electron transfer to semiconductors, respectively. For both cases, one must deal with a manifold of electronic states. In general, however, the FSSH algorithm has usually been restricted to studying isolated molecules in solvents with only a handful of electronic states.[38,68] Thus far, the most important exception to this general rule was the pioneering "Independent Electron Surface Hopping (IESH)" model of Shenvi, Roy, and Tully,[39–41] who studied NO scattering off of a gold surface. Shenvi *et al.* suggested discretizing a continuum of adiabatic electronic levels to simulate electronic friction in a metal; by running FSSH on a large number of electronic states, Shenvi *et al.* were able to correctly describe vibrational relaxation of the NO molecule. In a slightly different context, Preston and Cohen also proposed a "surface leaking" approach for treating the decay of an electronic state into a continuum of electronic levels but, to our knowledge, surface leaking has thus far only been applied to study loosely bound anions.[42,43]

In a companion paper,[72] we have discussed a straightforward extension of FSSH to treat model one-electron systems. In the present paper, we focus on a many-body problem and offer a simple (but generalizable) SH approach describing a molecule absorbed on a metal surface. We will study the simplest case: a single impurity level coupled to a single phonon as well as one or two electronic (fermionic) baths (which is known as the Anderson-Holstein model[44,45]). For the case of one electronic bath, we study relaxation to equilibrium. For the case of two electronic baths, with different Fermi levels, we will study the steady state transport, where some features of inelastic scattering are visible.[46,47] The approach in this paper will not rely on the assumption of small electron-phonon couplings and, as such, should go beyond standard models of electronic friction acting on molecules at metal surfaces.[48–50] Furthermore, in the future, it will be important to include a bath of external vibrations as well, which can be achieved easily through a random force in our surface (or, more formally, through a Fokker-Planck equation[51]). For the present article, we will restrict ourselves to the simple Anderson-Holstein model (without any explicit nuclear friction) and we will demonstrate the power of a SH approach to recover many dynamical phenomena for this simple system.

An outline of this paper is as follows. In Sec. II, we will present the necessary theory. First, we will motivate and justify our SH approach based on a classical master equation (CME) for the nuclear-electronic subsystem. We will do this both for the cases of equilibrium (one electronic bath) and

 

out-of-equilibrium (two electronic baths) dynamics. Second, for concreteness, we will then give a step-by-step flowchart for our SH algorithm. Third, we will discuss briefly quantum master equations (QME) and numerical renormalization group (NRG) theory, which represent alternative formalisms against which we can benchmark our dynamics. In Sec. III, we will present results showing the power of this simple model. We conclude in Sec. IV.

## II. THEORY

### A. Model Hamiltonian

The Anderson-Holstein Hamiltonian involves an electronic impurity level coupled to (i) a phonon degree of freedom, and (ii) a continuum of electronic levels. One can think of the impurity level as an atomic or molecular orbital that can either give an electron to or take an electron from a metal surface. A common example would be an anion near a charged metal surface, e.g., an electrochemical interface. We group the impurity and phonon together as the system ($H_s$), and the continuous levels of electrons to be the bath ($H_b$). The interaction between them ($H_c$) is bilinear:

$$H = H_s + H_b + H_c, \tag{1}$$

$$H_s = E_d d^+ d + g(a^+ + a)d^+ d + \hbar\omega(a^+ a + \tfrac{1}{2}), \tag{2}$$

$$H_b = \sum\nolimits_k (\epsilon_k - \mu) c_k^+ c_k, \tag{3}$$

$$H_c = \sum\nolimits_k V_k (c_k^+ d + d^+ c_k). \tag{4}$$

Here, $d^+$ ($d$), $a^+$ ($a$), $c_k^+$ ($c_k$) are creation (annihilation) operators on the impurity electron, phonon, and metal electrons, respectively. $E_d$ is the impurity energy level, $\omega$ is the frequency of the phonon, $g$ is the coupling between the impurity and the phonon. $\epsilon_k$ is an energy level of the bath, which has Fermi level $\mu$, and $V_k$ is the coupling between the impurity and the bath. The interaction between the impurity and bath determines the hybridization function $\Gamma$,

$$\Gamma(\epsilon) = 2\pi \sum_k |V_k|^2 \delta(\epsilon - \epsilon_k). \tag{5}$$

In the following, we will assume that $\Gamma$ is a constant (the wide band approximation). In developing a SH model of the Anderson-Holstein model, it will be convenient to replace $a^+$ and $a$ with the (dimensionless) position $x$ and momentum $p$ coordinates, so that the system Hamiltonian is written as

$$H_s = E_d d^+ d + \sqrt{2} g x d^+ d + \frac{1}{2}\hbar\omega(x^2 + p^2). \tag{6}$$

### B. Classical master equation

In a surface-hopping based description of semiclassical dynamics, the critical input is the choice of classical potential surfaces and the implementation of the surface hopping algorithm. Here, we work in the diabatic representation of the electronic state of the system. In this representation, $d^+ d$ is either 0 or 1, that is, the impurity can be either unoccupied (denoted as state 0) or occupied (state 1). The corresponding diabatic potential surfaces for the nuclei are

$$V_0(x) = \tfrac{1}{2}\hbar\omega x^2, \tag{7}$$

$$V_1(x) = \tfrac{1}{2}\hbar\omega x^2 + \sqrt{2} g x + E_d. \tag{8}$$

The basic premise of our SH approach is to model the electronic bath implicitly; all of the information required about it are the rate $\Gamma$ and the Fermi distribution. Furthermore, we treat the phonon degree of freedom classically. The classical motion is carried on the diabatic surfaces (Eq. (7) or (8)) while, in the spirit of the Franck-Condon picture (vertical transitions), the hopping events are assumed to take place at fixed nuclear position and momentum and are controlled by rates $\gamma_{0\to1}(x,p)$ and $\gamma_{1\to0}(x,p)$ as described below. The ensuing dynamics is encoded in a CME for the probability density of the system:[51]

$$\begin{aligned}\frac{\partial P_0(x,p)}{\partial t} &= \frac{\partial H_0(x,p)}{\partial x}\frac{\partial P_0(x,p)}{\partial p} \\ &\quad - \frac{\partial H_0(x,p)}{\partial p}\frac{\partial P_0(x,p)}{\partial x} \\ &\quad - \gamma_{0\to1} P_0(x,p) + \gamma_{1\to0} P_1(x,p),\end{aligned} \tag{9}$$

$$\begin{aligned}\frac{\partial P_1(x,p)}{\partial t} &= \frac{\partial H_1(x,p)}{\partial x}\frac{\partial P_1(x,p)}{\partial p} \\ &\quad - \frac{\partial H_1(x,p)}{\partial p}\frac{\partial P_1(x,p)}{\partial x} \\ &\quad + \gamma_{0\to1} P_0(x,p) - \gamma_{1\to0} P_1(x,p),\end{aligned} \tag{10}$$

where the potential on each surface (in dimensionless coordinates) is

$$H_\alpha = V_\alpha(x) + \frac{1}{2}\hbar\omega p^2, \alpha = 0, 1. \tag{11}$$

Here, $P_0(x,p)$ $\left(P_1(x,p)\right)$ is the probability density for the impurity level to be unoccupied (occupied) with the position and momentum of the oscillator to be $x$ and $p$; $P_0$ and $P_1$ satisfy the obvious normalization condition $\int dxdp\left(P_1(x,p) + P_0(x,p)\right) = 1$.

Next, consider the hopping rates. If the classical system interacts with a single electronic bath (a free electron metal) for a long enough time, it is expected to reach a thermal equilibrium compatible with the temperature and chemical potential of this metal. The simplest choice of hopping rates compatible with this requirement is

$$\gamma_{0\to1} = \frac{\Gamma}{\hbar} f(\Delta V), \tag{12}$$

$$\gamma_{1\to0} = \frac{\Gamma}{\hbar}\left(1 - f(\Delta V)\right), \tag{13}$$

$$\Delta V(x) = V_1(x) - V_0(x), \tag{14}$$

where $f$ is the Fermi function of the bath

$$f(z) = \frac{1}{1 + e^{\beta(z-\mu)}}. \tag{15}$$

Equations (9)–(15) recover the correct equilibrium in the limit of small $\Gamma$ (shown below). (The restriction to small $\Gamma$ reflects the fact that level broadening is disregarded in the dynamics postulated above. In Sec. II E, we describe a way to incorporate level broadening properly.)

Before solving the CME at equilibrium, we note that according to Eqs. (9) and (10), the unoccupied ($P_0(x,p)$) and occupied ($P_1(x,p)$) probability densities evolve under two processes: (i) motion of a nucleus along its respective surface and (ii) hopping between two potential surfaces. Equations (12)–(14) imply that the latter is determined by both (i) the potential difference between the two potential surfaces and (ii) the time scale $\Gamma$ for electron transfer between the impurity and the bath. Thus, according to the CME, there is never any explicit damping of the oscillator's velocity.

Let us now return the question of an analytical steady state. For the case of equilibrium, we can set $\mu = 0$, and a solution to Eqs. (9)–(10) is given by

$$P_0(x,p) = C\exp\left(-\frac{1}{2}\beta\hbar\omega(x^2+p^2)\right), \tag{16}$$

$$\begin{aligned} P_1(x,p) &= C\exp\left(-\frac{1}{2}\beta\hbar\omega(x^2+p^2) - \sqrt{2}\beta g x - \beta E_d\right) \\ &= C\exp\left(-\frac{1}{2}\beta\hbar\omega\left((x+\sqrt{2}g/\hbar\omega)^2+p^2\right)\right. \\ &\quad \left. - \beta(E_d - g^2/\hbar\omega)\right). \end{aligned} \tag{17}$$

$C$ is a normalization factor, determined by $\int\int dxdp\,(P_0(x,p)+P_1(x,p)) = 1$,

$$C = \frac{\beta\hbar\omega}{2\pi}\frac{1}{1+\exp(-\beta(E_d - g^2/\hbar\omega))}. \tag{18}$$

These solutions are just the simple Boltzmann distributions that one would expect in the limit of small $\Gamma$. The reduced distribution functions for the position $x$ and momentum $p$ of the oscillator, then take the forms

$$\begin{aligned} P(p) &= \int dx\Big(P_0(x,p)+P_1(x,p)\Big) \\ &= \sqrt{\frac{\beta\hbar\omega}{2\pi}}\exp(-\frac{1}{2}\beta\hbar\omega p^2), \end{aligned} \tag{19}$$

$$\begin{aligned} P(x) &= \int dp\Big(P_0(x,p)+P_1(x,p)\Big) \\ &= C\sqrt{\frac{2\pi}{\beta\hbar\omega}}\Big(\exp(-\frac{1}{2}\beta\hbar\omega x^2) \\ &\quad + \exp(-\frac{1}{2}\beta\hbar\omega x^2 - \sqrt{2}\beta g x - \beta E_d)\Big). \end{aligned} \tag{20}$$

Thus, assuming there is only one fixed point, we conclude that the CME with Eqs. (12) and (13) does capture the correct equilibrium for the case of one oscillator coupled to one bath.[52,69,70]

Obviously, Eqs. (12)–(15) can be generalized in a straightforward way to situations where the system is coupled to many electronic baths, each in its own equilibrium. For example, for a conduction junction comprising two metals, $L$ and $R$, Eqs. (12)–(13) are replaced by

$$\gamma_{0\to1} = \frac{\Gamma_L}{\hbar}f^L(\Delta V) + \frac{\Gamma_R}{\hbar}f^R(\Delta V), \tag{21}$$

$$\gamma_{1\to0} = \frac{\Gamma_L}{\hbar}(1-f^L(\Delta V)) + \frac{\Gamma_R}{\hbar}(1-f^R(\Delta V)), \tag{22}$$

where $f^L$ ($f^R$) is the Fermi function for left (right) bath with chemical potential $\mu_L$ ($\mu_R$) and $\Gamma_L$ ($\Gamma_R$) represents the corresponding left (right) hybridization.

Once the probability densities $P_\alpha(x,p;t)$ ($\alpha = 0,1$) have been determined, we can calculate just about any quantity of interest. For example, the population of the impurity level $N$ and the kinetic energy of the oscillator $E_k$ are

$$N = \int dxdpP_1(x,p), \tag{23}$$

$$E_k = \int dxdp\Big(P_1(x,p)+P_0(x,p)\Big)\tfrac{1}{2}\hbar\omega p^2. \tag{24}$$

For a biased conduction junction with $f^L \neq f^R$, the long time dynamics will converge to a non-equilibrium steady state characterized by the electronic current

$$I = \int dxdp\Big(\gamma^L_{0\to1}(x)P_0(x,p) - \gamma^L_{1\to0}(x)P_1(x,p)\Big) \tag{25}$$

with

$$\gamma^L_{0\to1} = \frac{\Gamma_L}{\hbar}f^L(\Delta V), \tag{26}$$

$$\gamma^L_{1\to0} = \frac{\Gamma_L}{\hbar}(1-f^L(\Delta V)). \tag{27}$$

### C. Surface hopping algorithm

The dynamics of Eqs. (9) and (10) can be solved directly using a simple SH approach. The algorithm is as follows:

1. Prepare the initial velocities and positions of the oscillators according to the relevant initial conditions. Note that these initial conditions will be irrelevant if one seeks only a description of equilibrium or steady state (and transient dynamics are not important). As discussed above, we believe the CME yields a unique fixed point at long times. In the present paper, we initialize all velocities and positions so that they satisfy a Boltzmann distribution at a given initial temperature on one potential surface,
$$P_0(x,p) = \frac{\beta\hbar\omega}{2\pi}\exp(-\tfrac{1}{2}\beta\hbar\omega(x^2+p^2)), \tag{28}$$
$$P_1(x,p) = 0. \tag{29}$$
2. At the beginning of every time step, if the oscillator is moving along surface $\alpha$ and has position $x$, determine the possibility of hopping $\gamma_{\alpha\to\alpha'}(x)$ in Eqs. (12) and (13) (or Eqs. (21) and (22) for two baths), and generate a random number $\xi \in [0,1]$. If $\xi < \gamma_{\alpha\to\alpha'}(x)dt$, then we switch surfaces (and the active surface becomes $\alpha'$); otherwise, we keep the same active surface.
3. Propagate the position $x$ and momentum $p$ along the active diabatic potential surface for a time step $dt$.
4. Repeat step 2 and sample over as long a trajectory as is desired until convergence. For dynamical averages, it will be necessary to sample over many independent trajectories.

The scheme above is visualized in Fig. 1. We emphasize again that, at step 2, if the oscillator hops, the momentum is not rescaled to conserve total nuclear energy. This variability in the energy of the oscillator is different from standard FSSH[1] (and resembles more "surface leaking"[42,43]); as will be shown,

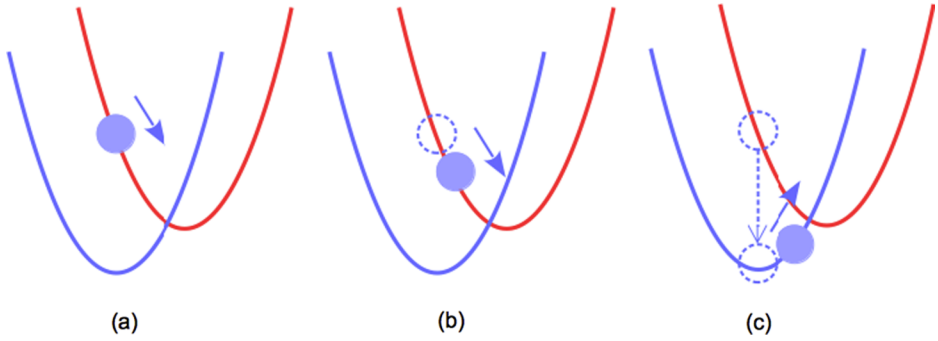


FIG. 1. How to run SH: We assume that the oscillator (blue ball) has been moving along on the red potential energy surface. (a) At the start of each time step, we generate a random number $\xi$. If $\xi > \gamma_{red\to blue}(x)dt$, (b), the oscillator will continue to move along the red potential energy surface for the next time interval $dt$. Otherwise, (c), the oscillator will jump and move along the blue surface for the next time interval $dt$.

this naive hopping scheme allows the nucleus to relax to the temperature of the electronic bath.

### D. Quantum master equation

The CME (Eqs. (9) and (10)) will not be adequate at low temperature where $kT < \hbar\omega$, and a quantum description of the oscillator is needed. In the limit of small $\Gamma$, such a description is provided by the QME,[53,54]

$$\frac{dP_q^n}{dt} = \sum_{n',q'} [P_{q'}^{n'} W_{q'\to q}^{n'\to n} - P_q^n W_{q\to q'}^{n\to n'}]. \tag{30}$$

Here, $P_q^n$ is the probability density for the impurity to be in electronic state $n$ ($|n\rangle = |0\rangle, |1\rangle$) and for the phonon to be in state $q$ ($|q\rangle = |0\rangle, |1\rangle, |2\rangle \ldots$). $W_{q\to q'}^{n\to n'}$ is the transition possibility from $n$ to $n'$ and $q$ to $q'$. For the case of one bath, $W_{q\to q'}^{n\to n'}$ is given by

$$W_{q\to q'}^{0\to 1} = \frac{\Gamma}{\hbar} |M_{q\to q'}|^2 f\left(E_d - \frac{g^2}{\hbar\omega} + \hbar\omega(q'-q)\right), \tag{31}$$

$$W_{q\to q'}^{1\to 0} = \frac{\Gamma}{\hbar} |M_{q\to q'}|^2 \left(1 - f(E_d - \frac{g^2}{\hbar\omega} + \hbar\omega(q-q')\right), \tag{32}$$

$$W_{q\to q'}^{n\to n'} = 0, n = n'. \tag{33}$$

Here, $E_d - \frac{g^2}{\hbar\omega}$ represents the renormalized energy level of the impurity (i.e., the energy of the impurity level minus the reorganization energy). $M_{q\to q'}$ is the Frank-Condon factor, which is the overlap between eigenstates $q$ and $q'$ of the harmonic oscillator with the origin shifted by $\sqrt{2}\lambda \equiv \sqrt{2}g/\hbar\omega$,

$$M_{q\to q'} = \int dx \phi_{q'}(x)\phi_q(x - \sqrt{2}\lambda). \tag{34}$$

The Franck-Condon factor can be expressed as[53,54]

$$M_{q\to q'} = (p!/Q!)^{1/2} \lambda^{Q-p} e^{-\lambda^2/2} L_p^{Q-p}(\lambda^2) \times sgn(p-Q)^{p-Q}. \tag{35}$$

Here, $Q(p)$ is the maximum (minimum) of $q$ and $q'$, $L_n^m$ is generalized Laguerre polynomial.

For the case of one bath, there is an analytical solution to Eqs. (30)–(33)

$$P_q^0 = C \exp(-\beta\hbar\omega(q + \frac{1}{2})), \tag{36}$$

$$P_q^1 = C \exp(-\beta\hbar\omega(q + \frac{1}{2})) \exp(-\beta(E_d - g^2/\hbar\omega)), \tag{37}$$

where C is the normalized factor that satisfies $\sum_q (P_q^0 + P_q^1) = 1$. This solution captures one oscillator in the presence of two possible electronic states (with small coupling $\Gamma$ between the states). Thus, the QME impurity population agrees exactly with the CME (compare Eqs. (36) and (37) with Eqs. (16) and (17)).

For the case of two baths, the hopping probability is the sum of the left and right hopping probabilities

$$W_{q'\to q}^{n\to n'} = W_{q'\to q}^{n\to n'^R} + W_{q'\to q}^{n\to n'^L}, \tag{38}$$

where $W_{q'\to q}^{n\to n'^R}$ ($W_{q'\to q}^{n\to n'^L}$) depend on the Fermi functions $f^R$ ($f^L$). At steady state, the impurity and the phonon can be collectively be described by $P_q^{n,ss}$, which is the normalized nontrivial solution to $\frac{dP_q^n}{dt} = 0\big|_{P_q^n = P_q^{n,ss}}$. $P_q^{n,ss}$ can be used to calculate any and all steady-state observables. For example, current is given by

$$I = \sum_{qq'} W_{q'\to q}^{0\to 1\ L} P_{q'}^{0,ss} - W_{q'\to q}^{1\to 0\ L} P_{q'}^{1,ss}. \tag{39}$$

When discussing our SH results below, we will compare with the QME results. For a QME simulation, we must truncate the infinite set of phonon states, including only a finite number, while making sure that the result is converged.

### E. Implementing level broadening

In conjunction with the equilibrium distribution Eqs. (16) and (17), Eq. (23) yields the equilibrium electron population of the impurity level predicted by the SH scheme in the form

$$N = \int dx dp P_1(x,p) = f(\tilde{E}_d), \tag{40}$$

where $\tilde{E}_d = E_d - g^2/\hbar\omega$ is impurity level energy renormalized by the reorganization energy $g^2/\hbar\omega$. Equation (40) is just a Fermi function at a well defined impurity energy, and thus Eq. (40) disregards level broadening. Indeed, in the case of no oscillators, the exact expression for the population of an impurity level (at energy $E_d$) interacting with an equilibrium Fermi distribution is given by[55]

$$N = \int dE \frac{1}{2\pi} \frac{\Gamma}{(E - E_d)^2 + (\Gamma/2)^2} f(E). \tag{41}$$

Consequently, Eq. (40) is a good approximation only in the limit of small impurity-bath coupling ($kT \gg \Gamma$). To improve upon this answer, one must fully account for the level broadening of the impurity by the electronic bath. Within the context of our SH calculations, we can include broadening as follows. For each trajectory in our simulation, we initialize the relative

energy level of the impurity $E_d$ according to a Lorentzian distribution,

$$\rho(E) = \frac{1}{2\pi}\frac{\Gamma}{(E-E_d)^2+(\Gamma/2)^2}. \tag{42}$$

Thereafter, we run many simulations, evaluating physical observables by averaging over all trajectories. For the electronic population of the impurity, we get

$$\begin{aligned} N &= \int dE\rho(E)f(E-g^2/\hbar\omega) \\ &= \int dE\frac{1}{2\pi}\frac{\Gamma}{(E-\tilde{E}_d)^2+(\Gamma/2)^2}f(E). \end{aligned} \tag{43}$$

Except for the shift of the impurity energy level ($\tilde{E}_d = E_d - g^2/\hbar\omega$ instead of $E_d$), Eq. (43) is the same as Eq. (41).

In Appendix A, we show how the level broadening changes the position $x$ and momentum $p$ distribution (Eqs. (19) and (20)). Furthermore, we define a mean potential and a potential of mean force, and show that, without taking the broadening into account ($\Gamma \ll kT$), these two potentials give the same result.

### F. Numerical renormalization group

Finally, it is important to remember that both the CME and QME methods above treat the electronic bath implicitly (and are derived only by assuming that $\Gamma$ is very small). In the end, the validity of our SH results needs to be justified. At equilibrium this can be done by comparing with results of a NRG[56,57] calculation, which, at low enough temperatures can yield very accurate results when converged properly.[58,71] This method is particularly suited for a system with small number of degrees of freedom interaction with a microscopic bath. By logarithmically discretizing the continuum representing the bath, the NRG approach transforms a Hamiltonian with a continuous number of system-bath couplings into a semi-infinite chain, where each site of the chain only couples with its nearest neighbors. Furthermore, because the couplings along the chain decrease exponentially, one can easily truncate the infinite Hilbert space representing the bath and recover very accurate answers. Details about NRG for bosons and fermions can be found in Refs. 56 and 57.

## III. RESULTS AND DISCUSSION

### A. One electronic bath–relaxation to equilibrium

For the problem of one electronic bath, we first investigate the relaxation of the oscillator towards equilibrium using the simplest SH scheme with rates given by Eqs. (12)–(15). Figure 2(a) shows the time evolution of the average kinetic energy of the oscillator for a variety of initial temperatures. For each initial condition, we find that the kinetic energy of the system inevitably reaches its classical thermal limit $E_K = \frac{1}{2}kT$ where $kT$ is the temperature of the electronic bath. The same long-time limit is obtained (Figure 2(b)) for different choices of the e-ph couplings $g$. Increasing the e-ph coupling causes faster relaxation but the final equilibrium state is unchanged.

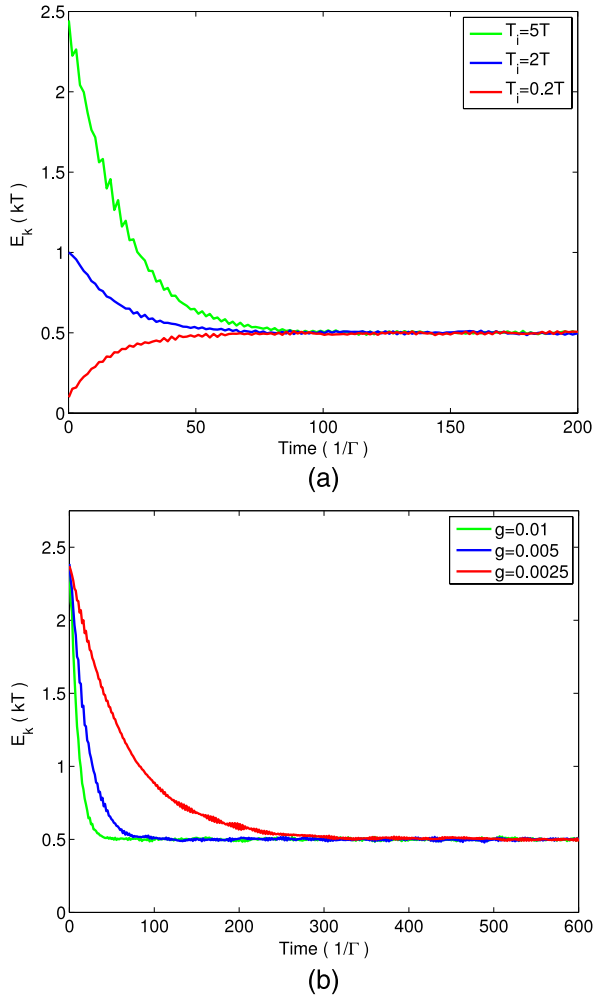


FIG. 2. Phonon relaxation: $\Gamma = 0.003$, $kT = 0.03$, $\hbar\omega = 0.003$, $E_d = 0$, $\mu = 0$. 10 000 trajectories are used. (a) Phonon relaxation with different initial conditions, g = 0.005. $T_i$ represents the temperature at which the oscillator is initialized. (b) Phonon relaxation with different e-ph couplings, $g$.

In Figure 3, we plot the numerical distributions of the oscillator position $x$ and momentum $p$ that are obtained from the SH trajectories, as well as the analytical $x$ and $p$ distributions given by Eqs. (19) and (20). We find perfect agreement, thus reinforcing our intuition that Eqs. (9) and (10) admit only one long time solution.

The results displayed in Figures 2 and 3 have used the SH algorithm that disregarded level broadening. Figure 4 shows the effect of including broadening as described in Sec. II E. With broadening, we find perfect agreement of the computed impurity equilibrium population between SH/QME results and NRG results. (Recall that SH and QME yield identical impurity populations; see Eqs. (36), (37), (16), and (17).)

Finally, in Figure 5, we plot SH (Eq. (43)) vs. NRG results for a difficult (nonclassical) quantum regime, where $\Gamma$, $\hbar\omega$, $g^2/\hbar\omega > kT$. Not surprisingly, in this regime, SH cannot quite recover the correct electron population as a function of the renormalized impurity energy level ($\tilde{E}_d$). This figure should be a reminder that there are equilibrium regimes where SH is not applicable. In general, for many problems of interest, the agreement between SH and NRG is quite strong.

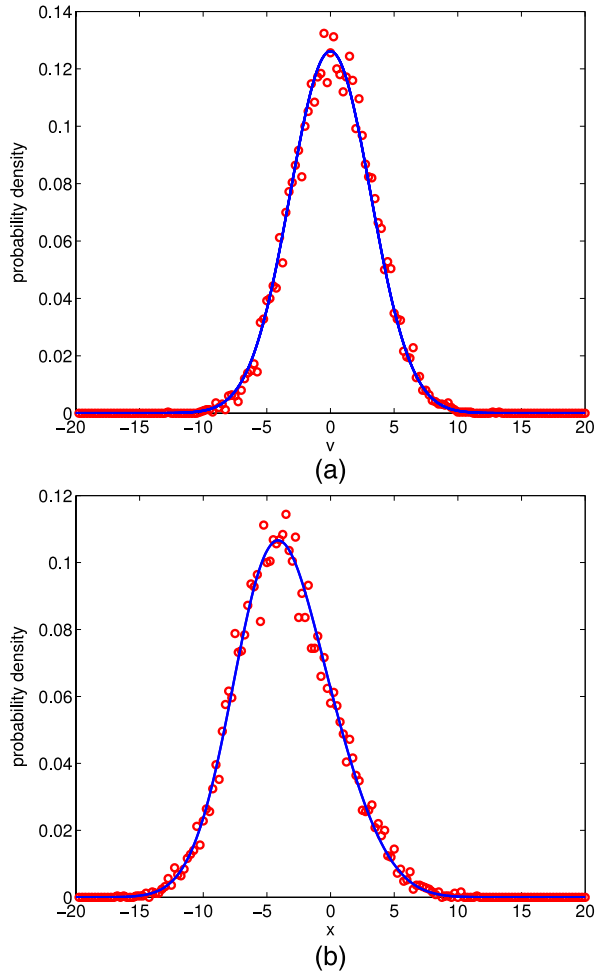


FIG. 3. Velocity distribution (a) and position distribution (b): $\Gamma = 0.003$, $kT = 0.03$, $g = 0.01$, $\hbar\omega = 0.003$, $E_d = 0$, $\mu = 0$. Red dots represent averages over 10 000 trajectories. The blue line is the analytic result from Eq. (19) for (a) and from Eq. (20) for (b). (a) Velocity distribution. (b) Position distribution.

### B. Two electronic baths–bias and current

The next system we investigated was the out of equilibrium case, where the Fermi levels of the two electronic baths have a bias between them. We calculated the current ($I$) as a function of bias ($V$). In the absence of e-ph coupling, the result is well known as single level Landauer formula from nonequilibrium Green Function approaches[59,60] and other frameworks,[61]

$$I = \int dE \frac{\Gamma_L \Gamma_R}{(E - E_d)^2 + (\Gamma/2)^2} (f^L(E) - f^R(E)), \quad (44)$$

where $\Gamma = \Gamma_L + \Gamma_R$.

In Figure 6, we plot the QME and SH results for current vs. voltage in the limit of very small e-ph coupling. For comparison, we also plot the Landauer current (Eq. (44), for which $g = 0$). For the SH results, we show both broadened and unbroadened results. In fact, it can be shown that, after broadening, SH gives the correct result compared with Eq. (44) (see Appendix B).

In Figure 6, we also show results from the QME, which should extend SH results into the limit of low temperature. According to Eqs. (31) and (32), just as for SH, the straightforward QME transition rates do not include broadening of the impurity levels. Just as for SH, however, we can include broadening by working with a series of different QME's (rather than just one), each with different impurity level energies sampled from Lorentzian distribution with half-width

$$\Gamma = \Gamma_L + \Gamma_R. \quad (45)$$

Having done so, we compute the current by averaging the QME results over the Lorentzian distribution of the impurity energy level $E_d$ (we sample over 5000 initial conditions for the simulation).

Note that all broadened methods (Landauer, QME, and SH) agree with each other in Fig. 6. Note also that, without broadening, neither the SH nor QME can reproduce the correct I-V curse. Thus, we may now have some confidence that, when broadening is included, SH can be extended to out of equilibrium case. We will next investigate the performance of the SH algorithm in the limits of larger electron-phonon couplings (which is the most interesting case).

In Figure 7, we calculate I-V curves at low temperature, comparing both the QME and real path integral results from Ref. 62. In this region, the quantum nature of the boson is paramount and SH must break down. We observe that the QME gets the correct overall form of the current in the quantum region, whereby the current should increase in steps at intervals of roughly $2\omega$.[46] From this agreement, we may conclude that the QME is valid at low or high temperatures.

In Figure 8, we compare our SH results with QME results as the temperature is raised. We observe that, in transitioning from the quantum (low T) region to the classical (high T)region, SH achieves better and better agreement with the QME. Although SH never captures a step feature at low temperature limit ($kT < \hbar\omega$) (where the energy levels of the nuclei are discretized), the SH approach is quite reliable at large temperatures.

Finally, Figure 9 compares I-V curves over a range of parameters going from the quantum limit to classical limit with and without broadening using different methods. Two general conclusions are apparent. First, broadening clearly reduces the step feature in the quantum limit. Second, with or without broadening, the QME and SH approaches agree in the classical limit. Overall, for future simulations of charge injection between classical fluids and metal surfaces, we expect that the SH approach discussed here should be quite reliable. In particular, even for systems with reasonable strong molecular-metal coupling, we are hopeful that SH can be applied, provided that we use the broadening protocol discussed above.

## IV. CONCLUSIONS

We have proposed a simple and effective way to treat coupled nuclear-electronic problems, and we have focused on the Anderson-Holstein model. The rules of our simulation are very simple: nuclear degrees of freedom are treated classically and evolve according to Newton's equation. Occasional hops between diabatic potential surfaces are promoted at a rate

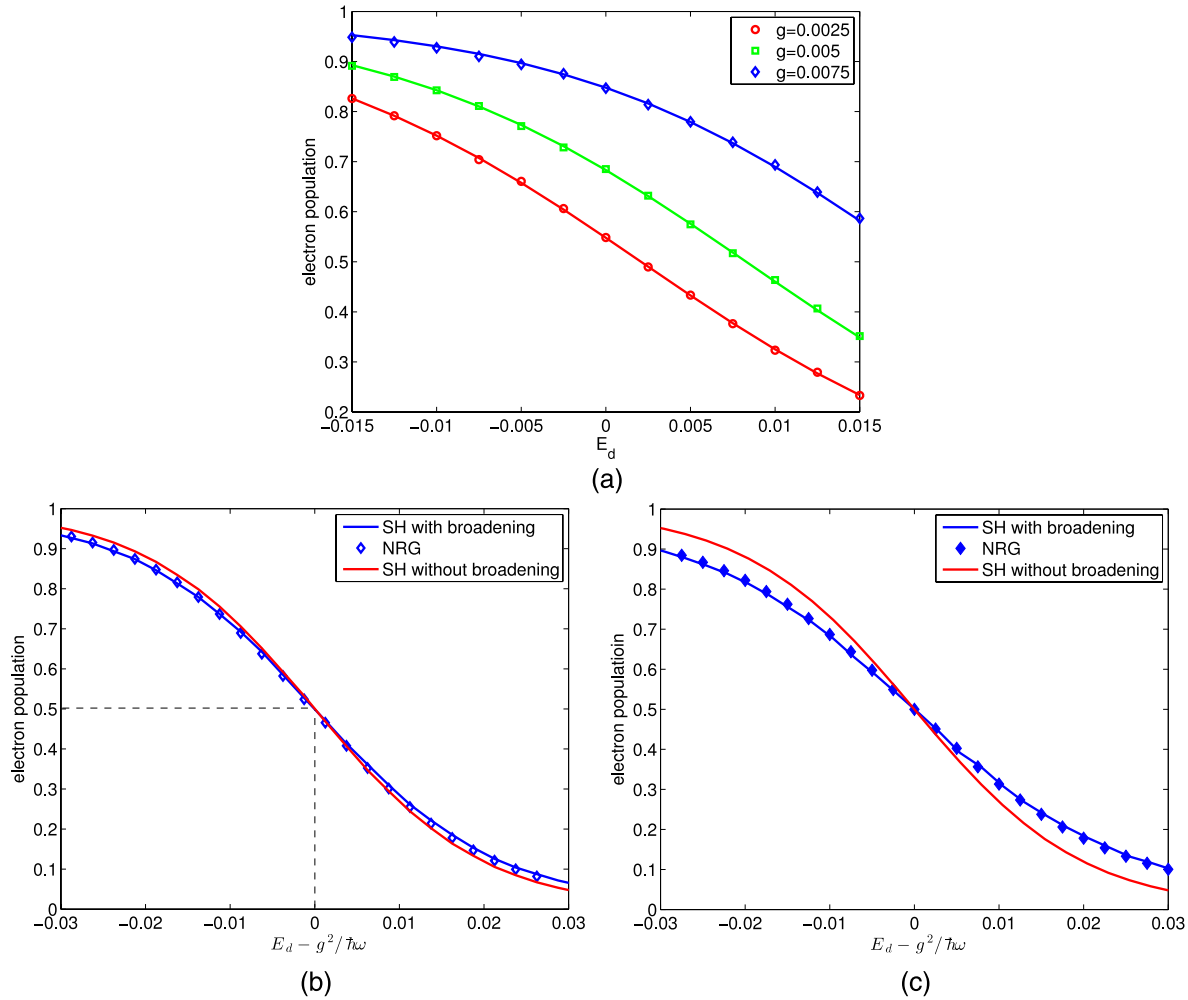


FIG. 4. Electronic population as a function of impurity energy level: $kT = 0.01$, $\hbar\omega = 0.003$. For NRG calculation, band width D = 1, and the basis is initialized with 30 boson states, the maximum number of eigenstates kept is $N_s = 512$, and the logarithmic discretizing parameter is $\Lambda = 2$. (a) Electron population of the impurity as a function of $E_d$. Dots represent the NRG results, the line represents the SH results when we include broadening. The agreement confirms the validity of our SH approach. $\Gamma = 0.003$. (b) Electron population as a function of shifted $E_d$, with $g = 0.0075$, $\Gamma = 0.003$. Note that, by including broadening, we do improve the SH results. (c) Electron population as a function of shifted $E_d$, with g = 0.0025, $\Gamma = 0.01$.

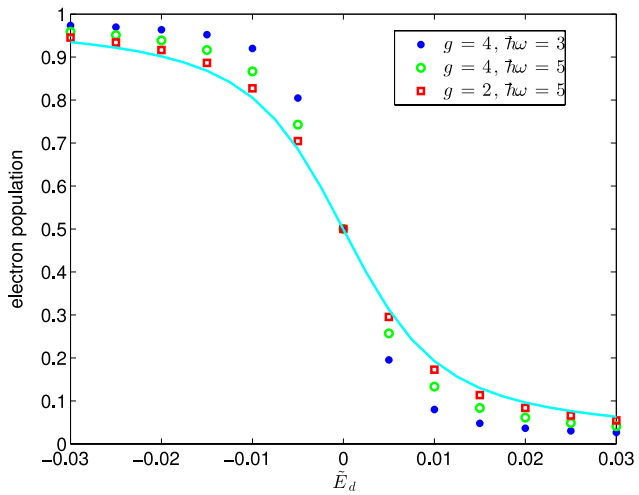


FIG. 5. Electronic population as a function of renormalized impurity energy level ($\tilde{E}_d = E_d - g^2/\hbar\omega$): $kT = 0.2\Gamma$, $\Gamma = 1$. The line represents SH results (Eqs. (43)), and the dots represent NRG results. For the NRG calculation, we set $D = 84\Gamma$, where D is the band width. The basis is initialized with 40 boson states, the maximum number of eigenstates kept is $N_s = 1500$, and the logarithmic discretizing parameter is $\Lambda = 2$.

proportional to the hybridization coupling between the system and the electronic bath.

For an impurity and phonon coupled to one electronic bath, we find that the system (impurity and phonon) recovers the correct thermal equilibrium regardless of any initial condition; the phonon learns about the temperature of the electronic bath indirectly (but effectively) through the hopping rate on and off. Interestingly, by broadening the energy level of the impurity (as induced by its interaction with the bath), we are able to recover the exact population of the impurity for all hybridizations in the limit of no electron-phonon coupling. Furthermore, with electron-phonon coupling, our results for the impurity electron population still yield good agreement with NRG calculations. As such, our final approach here would seem to go beyond any second order perturbation treatment of the impurity, for which there is not even any exact agreement without electron phonon coupling. That being said, we are aware, of course, that the standard CME or QME is derived from such a second-order perturbative treatment, and so the effect of our broadening will need to be tested more generally in the future.

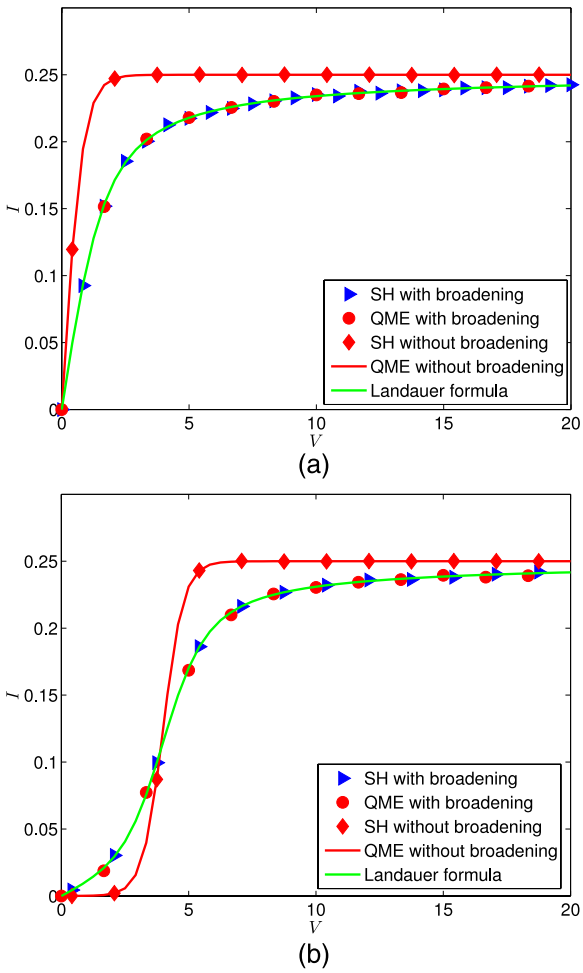


FIG. 6. I-V curves in the limit of small e-ph coupling. For the QME and SH, we take a small value for the e-ph coupling, $g = 0.02$. The other parameters are $kT = 0.2$, $\hbar\omega = 5$, $\Gamma = 2\Gamma_L = 2\Gamma_R = 1$, $\mu_L = V/2$, $\mu_R = -V/2$. The Landauer results are for $g = 0$ as in Eq. (44). (a) $E_d = 0$. (b) $E_d = 2$.

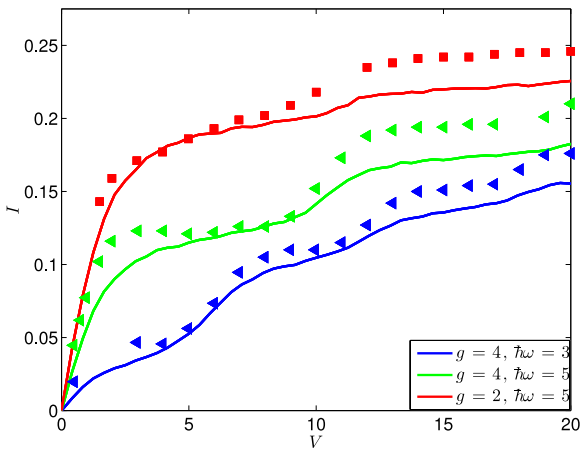


FIG. 7. I-V curves. The QME (as given by Eqs. (30)–(39) and broadened by Eqs. (42) and (45)) is represented by lines. Real time path integral results[62,63] are represented by dots. $kT = 0.2$. $\Gamma = 2\Gamma_L = 2\Gamma_R = 1$, $\mu_L = V/2$, $\mu_R = -V/2$, $E_d = g^2/\hbar\omega$. This choice of parameters represents the quantum regime, as can be seen by the non-linear steps in the I-V curve that arise from nuclear quantization. Our classical SH simulations will not be accurate in this regime.

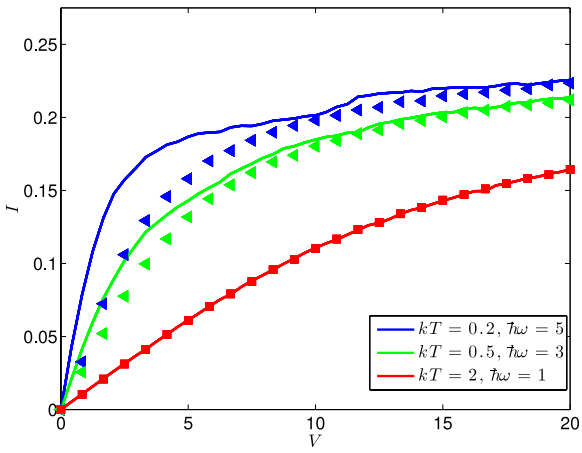


FIG. 8. I-V curves. Observe the agreement between SH (dots) and QME (lines) in the classical, high temperature limit. At low T, these two approaches disagree (as the QME predicts I-V steps, which SH ignores). $g = 2$, $\Gamma = 2\Gamma_L = 2\Gamma_R = 1$, $E_d = g^2/\hbar\omega$, $\mu_L = V/2$, $\mu_R = -V/2$.

For the out of equilibrium case, we have investigated both the CME and QME and explored high and low temperature regimes. As before, we have found improved results by broadening our master equation results. With broadening, both the CME and QME recover the Landauer formula (in the limit of zero e-ph coupling). At low temperature and for strong e-ph couplings, we have found that the QME recovers the correct step features in the I-V curves, whereas the CME fails. At high temperatures (in the classical limit), the SH and QME agree with each other.

Overall, we may conclude that the master equations presented here can be applied to physical problems that are either at equilibrium or out of equilibrium. In the future, we will aim to study a host of other interesting transport effects, including instability[54,64,65] and hysteresis.[46] Of course, in terms of cost, the SH approach is the least computationally demanding, followed by the QME, and then followed by NRG. Moreover, NRG would require a very large cost to propagate dynamics at high temperature.[66] Given the simplicity and efficiency of the SH approach here, one might expect that these dynamics will be very useful for simulating large systems of coupled classical nuclear degrees interacting with a reservoir of electrons, e.g., an electrochemical interface.[67] While further benchmarking of this method is undoubtedly needed, we believe the stochastic dynamics advocated in this paper will be a strong extension of the standard SH methodology.

## ACKNOWLEDGMENTS

We thank Charlie Epstein for fruitful conversations regarding the stability and uniqueness of solutions to master equations. J.E.S. thanks Guy Cohen and Misha Galperin for very useful conversations. This material is based upon work supported by the (U.S.) Air Force Office of Scientific Research (USAFOSR) PECASE award under AFOSR Grant No. FA9950-13-1-0157. J.E.S. acknowledges a Cottrell Research Scholar Fellowship and a David and Lucille Packard Fellowship.

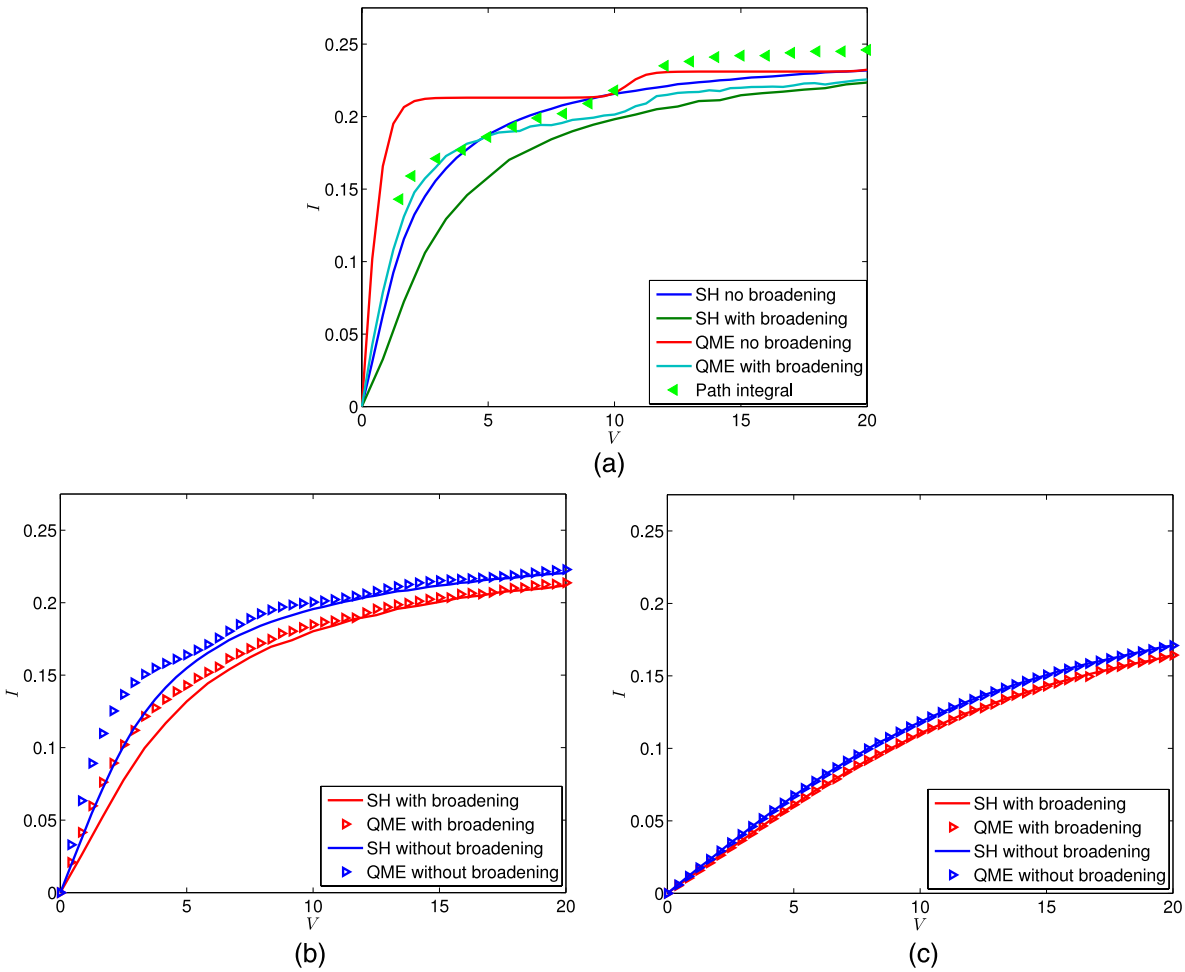


FIG. 9. I-V curves demonstrating the results from the different formalisms. The other parameters are $\Gamma = 2\Gamma_L = 2\Gamma_R = 1$, $\mu_L = V/2$, $\mu_R = -V/2$, $g = 2$. (a) $\hbar\omega = 5$, $kT = 0.2$ (b) $\hbar\omega = 3$, $kT = 0.5$. (c) $\hbar\omega = 1$, $kT = 2$.

## APPENDIX A: DYNAMICS WITH A BROADENED IMPURITY LEVEL: THE MEAN POTENTIAL AND THE POTENTIAL OF MEAN FORCE

The probability densities established in Eqs. (19) and (20) were computed without taking into account the broadening of the impurity energy level. After taking broadening into account as suggested above (Sec. II E), we must average over $E_d$, which is considered a variable with a Lorentzian distribution. $P(x)$ becomes

$$P(x) = \sqrt{\frac{2\pi}{\beta\hbar\omega}}\left((1-N)\exp(-\frac{1}{2}\beta\hbar\omega x^2) + N\exp(-\frac{1}{2}\beta\hbar\omega(x+\sqrt{2}g/\hbar\omega)^2)\right), \quad \text{(A1)}$$

with $N$ defined in Eq. (43). After averaging, $P(p)$ remains unchanged, as in Eq. (19), which indicates the average kinetic energy is still $\frac{1}{2}kT$. Using $P(x)$ above, we can define the mean potential,

$$P(x) = \exp(-\beta V_{MP}), \quad \text{(A2)}$$

which gives $V_{MP}$

$$V_{MP} = V_0 - \frac{1}{\beta}\log\left((1-N)\exp(-\frac{1}{2}\beta\hbar\omega x^2) + N\exp(-\frac{1}{2}\beta\hbar\omega(x+\sqrt{2}g/\hbar\omega)^2)\right), \quad \text{(A3)}$$

with $V_0 = -\frac{1}{\beta}\log\sqrt{\frac{2\pi}{\beta\hbar\omega}}$ is a constant.

Now, according to Ref. 48, the potential of mean force is defined as

$$V_{PMF} = \frac{1}{2}\hbar\omega x^2 - \int_{x_0}^{x} dx' F(x'). \quad \text{(A4)}$$

Here, the mean force $F(x)$ on the oscillator (as induced by the electrons) is defined as

$$F(x) = -\sqrt{2}g\langle d^+ d\rangle|_x = -\sqrt{2}g\int\frac{dE}{\pi}\frac{\Gamma}{(E-\sqrt{2}gx-E_d)^2+\Gamma^2}f(E). \quad \text{(A5)}$$

Let us now show that, if we exclude level broadening, Eqs. (A2) and (A4) give same result. Without broadening, using Eqs. (20) and (A2), the mean potential is

$$V_{MP} = V_1 - \frac{1}{\beta}\log\left(\exp(-\frac{1}{2}\beta\hbar\omega x^2) + \exp(-\frac{1}{2}\beta\hbar\omega x^2 - \sqrt{2}\beta g x - \beta E_d)\right)$$
$$= V_1 + \frac{1}{2}\hbar\omega x^2 - \frac{1}{\beta}\log(1+\exp(-\beta\sqrt{2}gx - \beta E_d)), \quad \text{(A6)}$$

where $V_1$ is a constant. Furthermore, the mean force defined in Eq. (A5) (without broadening) becomes

$$F(x) = -\sqrt{2}g\langle d^+ d\rangle|_x = -\sqrt{2}g f(\sqrt{2}gx + E_d). \quad \text{(A7)}$$

The integral over x gives the extra potential felt by the oscillator,

$$-\int_{x_0}^{x} dx' F(x') = \int_{x_0}^{x} \sqrt{2}g f(\sqrt{2}gx + E_d)$$
$$= V_2 - \frac{1}{\beta}\log(1+\exp(-\beta\sqrt{2}gx - \beta E_d)). \quad \text{(A8)}$$

$V_2$ is another constant reference potential. Thus, the potential of mean force is

$$V_{PMF} = V_2 + \frac{1}{2}\hbar\omega x^2 - \frac{1}{\beta}\log(1+\exp(-\beta\sqrt{2}gx - \beta E_d)). \quad \text{(A9)}$$

Within a constant, $V_{PMF} = V_{MP}$.

## APPENDIX B: CURRENT FROM SH IN ABSENT OF E-PH COUPLING

In this appendix, we show that (with broadening) our SH approach (as well as the QME) recovers the correct Landauer current in the limit of no electron-phonon coupling. In such a case, $P_1(x,p) = P_1, P_0(x,p) = P_0$. Both the CME (Eqs. (9) and (10)) and QME become

$$\frac{\partial P_0}{\partial t} = -\gamma_{0\to1}P_0 + \gamma_{1\to0}P_1, \quad \text{(B1)}$$
$$\frac{\partial P_1}{\partial t} = \gamma_{0\to1}P_0 - \gamma_{1\to0}P_1. \quad \text{(B2)}$$

Plugging in Eqs. (21) and (22), where now $\Delta V = E_d$, we find steady state solutions

$$P_0 = \frac{\Gamma_L(1-f^L(E_d)) + \Gamma_R(1-f^R(E_d))}{\Gamma}, \quad \text{(B3)}$$
$$P_1 = \frac{\Gamma_L f^L(E_d) + \Gamma_R f^R(E_d)}{\Gamma}. \quad \text{(B4)}$$

The current (Eq. (25)) is given by

$$I = \Gamma_L f^L(E_d)P_0 - \Gamma_L(1-f^L(E_d))P_1$$
$$= \frac{\Gamma_L\Gamma_R}{\Gamma}(f^L(E_d) - f^R(E_d)). \quad \text{(B5)}$$

Finally, when $E_d$ is broadened by a Lorentzian of width $\Gamma = \Gamma^L + \Gamma^R$, the result after averaging is

$$I = \int \frac{dE}{2\pi}\frac{\Gamma_L\Gamma_R}{(E-E_d)^2 + (\Gamma/2)^2}(f^L(E) - f^R(E)). \quad \text{(B6)}$$

This is the correct Landauer current.


[1] J. C. Tully, J. Chem. Phys. **93**, 1061 (1990).
[2] J. C. Tully and R. K. Preston, J. Chem. Phys. **55**, 562 (1971).
[3] O. V. Prezhdo and P. J. Rossky, J. Chem. Phys. **107**, 825 (1997).
[4] M. J. Bedard-Hearn, R. E. Larsen, and B. J. Schwartz, J. Chem. Phys. **123**, 234106 (2005).
[5] R. E. Larsen, M. J. Bedard-Hearn, and B. J. Schwartz, J. Phys. Chem. B **110**, 20055 (2006).
[6] J. Y. Fang and S. Hammes-Schiffer, J. Phys. Chem. A **103**, 9399 (1999).
[7] J. Y. Fang and S. Hammes-Schiffer, J. Chem. Phys. **110**, 11166 (1999).
[8] Y. L. Volobuev, M. D. Hack, M. S. Topaler, and D. G. Truhlar, J. Chem. Phys. **112**, 9716 (2000).
[9] M. D. Hack and D. G. Truhlar, J. Chem. Phys. **114**, 2894 (2001).
[10] A. W. Jasper, M. D. Hack, and D. G. Truhlar, J. Chem. Phys. **115**, 1804 (2001).
[11] C. Zhu, A. W. Jasper, and D. G. Truhlar, J. Chem. Phys. **120**, 5543 (2004).
[12] C. Zhu, S. Nangia, A. W. Jasper, and D. G. Truhlar, J. Chem. Phys. **121**, 7658 (2004).
[13] A. W. Jasper and D. G. Truhlar, J. Chem. Phys. **123**, 064103 (2005).
[14] F. Webster, P. J. Rossky, and R. A. Friesner, Comput. Phys. Commun. **63**, 494 (1991).
[15] F. Webster, E. T. Wang, P. J. Rossky, and R. A. Friesner, J. Chem. Phys. **100**, 4835 (1994).
[16] K. F. Wong and P. J. Rossky, J. Chem. Phys. **116**, 8418 (2002).
[17] K. F. Wong and P. J. Rossky, J. Chem. Phys. **116**, 8429 (2002).
[18] B. J. Schwartz, E. R. Bittner, O. V. Prezhdo, and P. J. Rossky, J. Chem. Phys. **104**, 5942 (1996).
[19] J. E. Subotnik and N. Shenvi, J. Chem. Phys. **134**, 024105 (2011).
[20] J. E. Subotnik and N. Shenvi, J. Chem. Phys. **134**, 244114 (2011).
[21] N. Shenvi, J. E. Subotnik, and W. Yang, J. Chem. Phys. **134**, 144102 (2011).
[22] B. R. Landry and J. E. Subotnik, J. Chem. Phys. **137**, 22A513 (2012).
[23] B. J. Schwartz and P. J. Rossky, J. Chem. Phys. **101**, 6917 (1994).
[24] A. S. Petit and J. E. Subotnik, J. Chem. Phys. **141**, 014107 (2014).
[25] T. Zimmermann and J. Vanicek, J. Chem. Phys. **141**, 134102 (2014).
[26] A. S. Petit and J. E. Subotnik, J. Chem. Phys. **141**, 154108 (2014).
[27] R. Tempelaar, C. P. van der Vegte, J. Knoester, and T. L. C. Jansen, J. Chem. Phys. **138**, 164106 (2013).
[28] J. E. Subotnik, W. Ouyang, and B. R. Landry, J. Chem. Phys. **139**, 214107 (2013).
[29] R. Kapral and G. Ciccotti, J. Chem. Phys. **110**, 8919 (1999).
[30] C. C. Martens and J. Y. Fang, J. Chem. Phys. **106**, 4918 (1997).
[31] Q. Shi and E. Geva, J. Chem. Phys. **121**, 3393 (2004).
[32] P. Huo and D. Coker, J. Chem. Phys. **137**, 22A535 (2012).
[33] F. Sterpone, M. J. Bedard-Hearn, and P. J. Rossky, J. Phys. Chem. A **113**, 3427 (2009).
[34] A. Hazra, A. V. Soudakov, and S. Hammes-Schiffer, J. Phys. Chem. B **114**, 12319 (2010).
[35] D. Nachtigallova, A. J. A. Aquino, J. J. Szymczak, M. Barbatti, P. Hobza, and H. Lischka, J. Phys. Chem. A **115**, 5247 (2011).
[36] T. Nelson, S. Fernandez-Alberti, A. E. Roitberg, and S. Tretiak, Acc. Chem. Res. **47**, 1155 (2014).
[37] R. Long and O. V. Prezhdo, J. Am. Chem. Soc. **136**, 4343 (2014).
[38] Li *et al.* recently explored a scheme for mixing FSSH dynamics with mean-field Ehrenfest dynamics to handle the particular case of one well-defined ground state interacting with a manifold of excited states.[68]
[39] N. Shenvi, S. Roy, and J. C. Tully, J. Chem. Phys. **130**, 174107 (2009).
[40] N. Shenvi, S. Roy, and J. C. Tully, Science **326**, 829 (2009).
[41] N. Shenvi, J. R. Schmidt, S. T. Edwards, and J. C. Tully, Phys. Rev. A **78**, 022502 (2008).
[42] R. K. Preston and J. S. Cohen, J. Chem. Phys. **65**, 15891 (1976).
[43] N. Sisourat, J. Chem. Phys. **139**, 074111 (2013).
[44] P. W. Anderson, Phys. Rev. **124**, 41 (1961).
[45] T. Holstein, Ann. Phys. **8**, 325 (1959).
[46] M. Galperin, M. A. Ratner, and A. Nitzan, J. Phys: Condens. Matter **19**, 103201 (2007).
[47] M. Galperin, M. A. Ratner, and A. Nitzan, Nano Lett. **5**, 125 (2005).
[48] N. Bode, S. V. Kusminskiy, R. Egger, and F. von Oppen, Beilstein J. Nanotechnol. **3**, 144 (2012).
[49] M. Brandbyge, P. Hedegård, T. F. Heinz, J. A. Misewich, and D. M. Newns, Phys. Rev. B **52**, 6042 (1995).
[50] M. Head-Gordon and J. C. Tully, J. Chem. Phys. **103**, 10137 (1995).
[51] F. Elste, G. Weick, C. Timm, and F. V. Oppen, Appl. Phys. A: Mater. Sci. Process. **93**, 345 (2008).
[52] Interestingly, for standard Tully style FSSH, detailed balance is also recovered–but only approximately (usually up to a small factor).[69,70] For the CME, the detailed balance is in fact exact in the limit of $\Gamma \to 0$.

[53]J. Koch, F. von Oppen, Y. Oreg, and E. Sela, Phys. Rev. B **70**, 195107 (2004).
[54]J. Koch, M. Semmelhack, F. von Oppen, and A. Nitzan, Phys. Rev. B **73**, 155306 (2006).
[55]H. Bruus and K. Flensberg, *Many-Body Quantum Theory in Condensed Matter Physics: An Introduction* (Oxford University Press, 2004).
[56]R. Bulla, T. A. Costi, and T. Pruschke, Rev. Mod. Phys. **80**, 395 (2008).
[57]K. G. Wilson, Rev. Mod. Phys. **47**, 773 (1975).
[58]Another option would be to compare our results against MCTDH (multi-configuration time-dependent Hartree) calculations.[71]
[59]H. Haug and A. Jauho, *Quantum Kinetics in Transport and Optics of Semiconductors* (Springer, New York, 2007).
[60]J. E. Subotnik, T. Hansen, M. A. Ratner, and A. Nitzan, J. Chem. Phys. **130**, 144105 (2009).
[61]D. Segal and A. Nitzan, Chem. Phys. **268**, 315 (2001).
[62]L. Mühlbacher and E. Rabani, Phys. Rev. Lett. **100**, 176403 (2008).
[63]The data is tracked from Ref. 62 using Data Tracker. In the paper, $E_d = 0$, but it seems the renormalized impurity level should be 0, that is $E_d - g^2/\hbar\omega = 0$.
[64]K. Kaasbjerg, T. Novotný, and A. Nitzan, Phys. Rev. B **88**, 201405 (2013).
[65]L. Siddiqui, A. W. Ghosh, and S. Datta, Phys. Rev. B **76**, 085433 (2007).
[66]F. B. Anders and A. Schiller, Phys. Rev. Lett. **95**, 196801 (2005).
[67]G. Floß, G. Granucci, and P. Saalfrank, J. Chem. Phys. **137**, 234701 (2012).
[68]S. A. Fischer, C. T. Chapman, and X. Li, J. Chem. Phys. **135**, 144102 (2011).
[69]J. R. Schmidt, P. V. Parandekar, and J. C. Tully, J. Chem. Phys. **129**, 044104 (2008).
[70]P. V. Parandekar and J. C. Tully, J. Chem. Phys. **122**, 094102 (2005).
[71]M. Thoss, I. Kondov, and H. Wang, Phys. Rev. B **76**, 153313 (2007).
[72]W. Ouyang, W. Dou, and J. Subotnik, J. Chem. Phys. **142**, 084109 (2015).